in solution is in fact suggested by the reversible color change from the reddish brown to the emerald green and vice versa, observed when a toluene solution of **5** is warmed (60 °C) and cooled (room temperature) during several cycles. We believe that the dissociation of dinitrogen leads to a quite reversible molecular reorganization where the monomeric **6** is formed as the main component of the product distribution. However the formation of unknown byproducts should necessarily be admitted. In agreement with the supposed high thermodynamic stability of complex **6**, attempts to prepare coordinatively unsaturated, N_2-free, highly reactive species, carried out by repeating the preparation of **5** under argon atmosphere, led only to variable amounts of **6** in spite of the careful stoichiometry control.

The crystal structure of **6** showed the compound as composed of two crystallographically independent and chemically equivalent monomeric molecules. The overall molecular geometry is shown in Figure 2. Even in this case, the vanadium atom is positioned on an inversion center of a highly symmetrical octahedron with the two pyridine molecules in trans positions. The values of the V-N distances are significantly different for the two unequivalent nitrogen atoms of the pyridine and Mz ligands [V-N21 = 2.241 (3) Å; V-N11 = 2.335 (3) a] as a result of the different nature of the bonding to vanadium. The V-C distance [V-C11 = 2.233 (4) Å] compares well with those found in the homoleptic $Li_4(Et_2O)_4VPh_6$.[5f]

Further work to investigate this point and to define the chemical reactivity of these V(II) complexes as well as synthetic efforts to prepare isostructural Ti derivatives is in progress at the moment.

Acknowledgment. Part of the X-ray work (A.L.S. and W.J.J.S.) has been supported by the Netherlands Foundation for Chemical Research (SON) with financial aid from the Netherlands Organization for Scientific Research (NWO). The data for **6** were collected by A. J. M. Duisenberg.

Supplementary Material Available: Tables with numerical details of the structure determination, hydrogen atom positions, thermal parameters, bond distances, and bond angles for **1** and **6** and a table of torsion angles for **6** (13 pages); listings of observed and calculated structure factors (32 pages). Ordering information is given on any current masthead page.

Contribution from the Departments of Chemistry, State University of New York at Buffalo, Buffalo, New York 14214, and University of California, Irvine, California 92717

Synthesis, Characterization, and X-ray Crystal Structure of $[Ru(NO_2)(PMe_3)_2(trpy)](ClO_4)$

Randolph A. Leising,[†] Stephen A. Kubow,[†] Melvyn Rowen Churchill,[†] Lisa A. Buttrey,[†] Joseph W. Ziller,[‡] and Kenneth J. Takeuchi*,[†]

Received July 19, 1989

The complex *trans*-$[Ru(NO_2)(PMe_3)_2(trpy)](ClO_4)$ (where trpy = 2,2':6',2''-terpyridine and PMe_3 = trimethylphosphine), has been prepared by using a five-step synthesis, starting from $RuCl_3 \cdot 3H_2O$, with a total overall yield of 27%. In addition, a three-step synthesis for the formation of *trans*-$[Ru(NO_2)(PMe_3)_2(trpy)](ClO_4)$ was developed, where an increase in the total overall yield from 27% to 71% was observed. Characterization of *trans*-$[Ru(NO_2)(PMe_3)_2(trpy)](ClO_4)$ was accomplished through UV-visible, IR, and ^1H and ^{13}C NMR spectroscopies, cyclic voltammetry, coulometry, and elemental analysis. An X-ray crystallographic structural determination was also performed, where *trans*-$[Ru(NO_2)(PMe_3)_2(trpy)](ClO_4)$ crystallized in the monoclinic space group $P2_1/c$ with cell parameters of a = 16.102 (11) Å, b = 10.365 (7) Å, c = 16.788 (12) Å, β = 108.23 (5)°, and Z = 4. Final discrepancy indices were R_F = 7.1% and R_{wF} = 6.4% for all 3169 nonzero data and R_F = 4.2% and R_{wF} = 5.1% for those 2186 reflections with $|F_o| > 6\sigma(|F_o|)$. The ruthenium to nitrogen bond distances were Ru-N(nitro) = 2.074 (6) Å and Ru-N(trpy) = 2.088 (6), 1.985 (5), and 2.093 (7) Å. The ruthenium to phosphorus bond distances were Ru-P = 2.361 (3) and 2.368 (3) Å.

Introduction

There has been considerable interest in ruthenium complexes that contain tertiary phosphine ligands, due to the well-documented use of low-valent ruthenium complexes in the area of homogeneous catalysis.[1-11] The chemistry of high-valent ruthenium complexes has also received much attention, in light of the potent oxidizing ability of these species.[12-17] Our research has been directed toward the utilization of tertiary phosphine ligands with high-oxidation-state ruthenium centers, where we have synthesized and characterized high-oxidation-state ruthenium complexes containing tertiary phosphine ligands. The phosphine ligands confer interesting properties on (oxo)ruthenium(IV) complexes[18-20] and on *trans*-$[Ru(NO_2)(PMe_3)_2(trpy)](ClO_4)_2$,[21] where both the stability and reactivity of these complexes are strongly affected by the phosphine ligands. For example, both the rates of substrate oxidation by (oxo)(phosphine)ruthenium(IV) complexes[22] and the resulting product distributions[23] depend on the ligand environment of the ruthenium complexes. Furthermore, linear rate enhancements were observed, based on the hydrophobicity of the substrate, for the oxidation of primary alcohols in water with these (oxo)(tertiary phosphine)ruthenium(IV) complexes.[22,24] Recently, we reported the synthesis and characterization of the first stable (nitro)ruthenium(III) complex, *trans*-$[Ru(NO_2)(PMe_3)_2$-

[†] State University of New York at Buffalo.
[‡] University of California.

(1) VanSickle, D. E.; Mayo, F. R.; Arluck, R. M. *J. Am. Chem. Soc.* **1965**, *87*, 4824.
(2) Hallman, P. S.; McGarvey, B. R.; Wilkinson, G. *J. Chem. Soc. A* **1968**, 3143.
(3) James, B. R. *Inorg. Chim. Acta Rev.* **1970**, *4*, 73.
(4) Cenini, S.; Fusi, A.; Capparella, G. *Inorg. Nucl. Chem. Lett.* **1972**, *8*, 127-131.
(5) James, B. R.; Wang, D. K. W.; Voigt, R. F. *J. Chem. Soc., Chem. Commun.* **1975**, 574-575.
(6) Dobson, A.; Robinson, S. D. *Inorg. Chem.* **1977**, *16*, 137-142.
(7) Sanchez-Delgado, R. A.; deOchoa, O. L. *J. Mol. Catal.* **1979**, *6*, 303-306.
(8) Riley, D. P.; Shumate, R. E. *J. Am. Chem. Soc.* **1984**, *106*, 3179-3184.
(9) Sanchez-Delgado, R. A.; Valencia, N.; Marquez-Silva, R.-L.; Andriollo, A.; Medina, M. *Inorg. Chem.* **1986**, *25*, 1106-1111.
(10) Leising, R. A.; Takeuchi, K. J. *Inorg. Chem.* **1987**, *26*, 4391-4393.
(11) Leising, R. A.; Ohman, J. S.; Takeuchi, K. J. *Inorg. Chem.* **1988**, *27*, 3804-3809.
(12) Moyer, B. A.; Meyer, T. J. *Inorg. Chem.* **1981**, *20*, 436-444.
(13) Carlsen, P. H. J.; Katsuki, T.; Martin, V. S.; Sharpless, K. B. *J. Org. Chem.* **1981**, *46*, 3936-3938.
(14) Thompson, M. S.; Meyer, T. J. *J. Am. Chem. Soc.* **1982**, *104*, 4106-4115.
(15) Gulliver, D. L.; Levason, W. *Coord. Chem. Rev.* **1982**, *46*, 1-127.
(16) Che, C. M.; Leung, W. H. *J. Chem. Soc., Chem. Commun.* **1987**, 1376.
(17) Seok, W. K.; Meyer, T. J. *J. Am. Chem. Soc.* **1988**, *110*, 7358-7367.
(18) Marmion, M. E.; Takeuchi, K. J. *J. Am. Chem. Soc.* **1986**, *108*, 510-511.

0020-1669/90/1329-1306$02.50/0

$(trpy)](ClO_4)_2$, where it was found that trans-phosphine ligands in combination with 2,2′:6′,2″-terpyridine were important in the stabilization of the (nitro)ruthenium(III) center. This ligand system allowed us to isolate the first example of a (nitro)ruthenium(III) complex that was stable both in the solid state and in solution.[21]

In response to a lack of reported synthetic methodology regarding the preparation of (nitro)(trans-phosphine)ruthenium complexes, we wish to report the synthesis and characterization of *trans*-$[Ru(NO_2)(PMe_3)_2(trpy)](ClO_4)$, which is the reduced form of *trans*-$[Ru(NO_2)(PMe_3)_2(trpy)](ClO_4)_2$. The synthesis involves five steps, starting with $RuCl_3 \cdot 3H_2O$. Included in our synthetic discussion is a one-pot method for introducing two trimethylphosphine ligands into trans positions of the coordination sphere of ruthenium. The characterization of *trans*-$[Ru(NO_2)(PMe_3)_2(trpy)](ClO_4)$ includes conductivity, coulometry, cyclic voltammetry, IR, UV–visible, ^1H NMR, and ^{13}C NMR spectroscopies, and an X-ray crystallographic structural determination.

Experimental Section

Materials. $RuCl_3 \cdot 3H_2O$ was purchased from Johnson Matthey Inc. 2,2′:6′,2″-Terpyridine was purchased from G. F. Smith Chemical Co. Trimethylphosphine was purchased from Aldrich Chemical Co. (0.1 M trimethylphosphine in toluene) and Strem Chemical. All of the above compounds were used as received. CH_3CN and CH_2Cl_2 were obtained from Fisher Scientific and were distilled from CaH_2. Reagent grade methanol was dried by distilling over Mg metal. All aqueous reactions used house distilled water, which was passed through Barnstead HN combination (No. D8922) and HN organic removal (No. D8904) purification cartridges before use. All other solvents, acids, bases, salts, and other materials were of reagent quality and were used without further purification.

Measurements. Elemental analyses were performed by Atlantic Microlabs (Norcross, GA). Infrared spectra were recorded with a Perkin-Elmer 1430 ratio recording infrared spectrophotometer, using thin film or Nujol mulls on NaCl plates. Measurements for the isotopic labelling study were made on a Mattson Cygnus 100 FT-infrared spectrometer, equipped with a Hewlett-Packard HP 7475A plotter, using diffuse reflectance techniques, with the sample distributed in powdered KBr. ^1H and ^{13}C NMR spectra were obtained on the JEOL FX-90Q FT spectrometer. All spectra were obtained by using deuterated chloroform as the solvent, with Me_4Si as the reference for the ^1H NMR spectra, and the ^{13}C NMR spectra used the center line of the $CDCl_3$ resonance, at 77.0 ppm, as the reference. UV–visible electronic spectra were obtained on a Bausch and Lomb Spectronic 2000 spectrophotometer equipped with a Houston Instrument Model 200 recorder. Cyclic voltammetric and coulometric measurements were obtained with an IBM EC/225 voltammetric analyzer, and the current–potential waves were recorded with a Houston Instruments Model 100 recorder. The cyclic voltammetric experiments were performed in a three-electrode, one-compartment cell, equipped with a platinum working electrode (Bioanalytical Systems), a platinum auxiliary electrode, and a saturated sodium chloride calomel (SSCE) reference electrode. Electrochemical measurements in CH_2Cl_2 used 0.1 M tetra-*n*-butylammonium tetrafluoroborate (Bu_4NBF_4) as the supporting electrolyte, while measurements in CH_3CN used 0.1 M tetraethylammonium perchlorate (TEAP) as the supporting electrolyte. The coulometric experiment was accomplished in a two-compartment, three-electrode, fritted cell with a platinum-gauze working electrode, a platinum auxiliary electrode, and an SSCE reference electrode and was conducted at ice temperatures. Coulombs were measured from the area under a current versus time plot recorded on the time-base drive of the Houston Instrument Model 200 recorder. Conductivity measurements were accomplished in distilled acetonitrile by using the method of Feltham and Hayter,[25] over a concentration range of 1.5–15 mM. Measurements were made with a YSI Model 31 conductivity bridge.

Collection of X-ray Diffraction Data. A single crystal of approximate dimensions 0.1 × 0.1 × 0.2 mm was mounted in a thin-walled glass capillary and aligned on a Syntex $P2_1$ automated four-circle diffractometer at the University at Buffalo-SUNY. Laue symmetry determination, crystal class, unit cell parameters, and the crystal's orientation matrix were carried out by previously described techniques.[26] Room-temperature (23 °C) intensity data were collected by using the θ–2θ scan technique with Mo Kα radiation under the conditions given in Table IV. All 3902 data were corrected for Lorentz and polarization effects and placed on an approximately absolute scale by means of a Wilson plot. A series of ψ scans of close-to-axial reflections showed less than 3% changes in transmission; no absorption correction was necessary. A careful survey of a preliminary data set revealed the systematic extinctions $0k0$ for $k = 2n + 1$ and $h0l$ for $l = 2n + 1$; the diffraction symmetry was $2/m$. The centrosymmetric monoclinic space group $P2_1/c$ [C_{2h}^5; No. 14] is thus uniquely defined.

Solution and Refinement of the Crystal Structure. All crystallographic calculations were carried out with either the UC Irvine modified version of the UCLA Crystallographic Computing Package[27] or the SHELXTL PLUS program set.[28] The analytical scattering factors for neutral atoms were used throughout the analysis;[29a] both the real ($\Delta f'$) and imaginary ($i\Delta f''$) components of anomalous dispersion were included.[29b]

The structure was solved by direct methods (SHELXTL PLUS); the positions of the ruthenium and phosphorus atoms were located from an *E* map. Subsequent difference-Fourier syntheses revealed the positions of all remaining non-hydrogen atoms. Full-matrix least-squares refinement of positional and thermal parameters (anisotropic for all non-hydrogen atoms) led to convergence with $R_F = 7.1\%$, $R_{wF} = 6.4\%$ and GOF = 1.01 for 316 variables refined against all 3169 unique data with $F_o > 0$ ($R_F = 5.3\%$;, $R_{wF} = 5.9\%$ for those 2589 data with $|F_o| > 3.0\sigma(|F_o|)$; $R_F = 4.2\%$, $R_{wF} = 5.1\%$ for those 2186 data with $|F_o| > 6.0\sigma(|F_o|)$). All hydrogen atoms were included in calculated positions (C–H = 0.96 Å and $U = 0.08$ Å^2) and were updated as refinement continued. A final difference-Fourier synthesis showed no significant features.

Synthesis. $RuCl_3(trpy)$. The starting material was prepared using modifications of a published method.[30a] A 0.653-g (2.50-mmol) sample of $RuCl_3 \cdot 3H_2O$ and 0.583 g (2.50 mmol, 1 equiv) of 2,2′:6′,2″-terpyridine were combined in 50 mL of MeOH (distilled over Mg). The mixture was heated at reflux under N_2 for 3 h and allowed to cool to room temperature, after which the solution was cooled in an ice bath for 0.5 h. The brown solid was collected by vacuum filtration, washed with cold MeOH until the filtrate was colorless, and then washed 4 times with Et_2O and air-dried. A total of 1.011 g of product (2.29 mmol, yield: 92%) was obtained, which was used without purification.

***trans*-$[RuCl_2(PMe_3)(trpy)]$.** A 0.200-g (0.454-mmol) sample of $RuCl_3(trpy)$ and 1.5 equiv (0.052 g, 0.681 mmol) of PMe_3 were combined in 60 mL of N_2-outgassed CH_2Cl_2. Then, 3 mL of NEt_3 (90 equiv, 40.8 mmol), or 5.0 g of Zn(Hg), were added to the solution. The solution was heated at reflux for 1.5 h and then filtered warm, and the filtrate was eluted through a deactivated alumina column (1.0 mL of H_2O per 10 mL of alumina), using CH_2Cl_2 as the eluent. The volume of the eluant was reduced with a rotary evaporator, the sample was triturated in hexanes, and the analytically pure product was collected by vacuum filtration. A total of 0.076 g (0.158 mmol) of purple product was collected; yield 43%. Anal. Calcd for $C_{18}H_{20}Cl_2N_3P_2Ru$: C, 44.90; H, 4.19. Found: C, 44.87; H, 4.20.

***cis*-$[RuCl_2(PMe_3)(trpy)]$.** A 0.070-g (0.146-mmol) sample of trans-$[RuCl_2(PMe_3)(trpy)]$ was added to 50 mL of CH_2Cl_2. The solution was irradiated with a 120 W tungsten light under N_2 for 4 h. The solvent was removed with a rotary evaporator, and the residue was dissolved in CH_2Cl_2 and then triturated in hexanes. A quantitative yield of *cis*-$[RuCl_2(PMe_3)(trpy)]$ was obtained. Anal. Calcd for $C_{21}H_{29}Cl_2N_3O_4P_2Ru$: C, 44.90; H, 4.19. Found: C, 44.84; H, 4.28.

Caution! While we have used perchlorate as a counter ion with a number of ruthenium(II) complexes without incident, perchlorate salts of metal complexes with organic ligands are potentially explosive. Care should be exercised in using a spatula or stirring rod to mechanically agitate any solid perchlorate. These complexes, as well as any other

(19) Marmion, M. E.; Takeuchi, K. J. *J. Am. Chem. Soc.* **1988**, *110*, 1472–1480.
(20) Kubow, S. A.; Marmion, M. E.; Takeuchi, K. J. *Inorg. Chem.* **1988**, *27*, 2761–2767.
(21) Leising, R. A.; Takeuchi, K. J. *J. Am. Chem. Soc.* **1988**, *110*, 4079–4080.
(22) Marmion, M. E.; Takeuchi, K. J. *J. Chem. Soc., Dalton Trans.* **1988**, 2385–2391.
(23) Marmion, M. E.; Leising, R. A.; Takeuchi, K. J. *J. Coord. Chem.* **1988**, *19*, 1–16.
(24) Marmion, M. E.; Takeuchi, K. J. *J. Chem. Soc., Chem. Commun.* **1987**, 1396–1397.
(25) Feltham, R. D.; Hayter, R. G. *J. Chem. Soc.* **1964**, 4587–4591.
(26) Churchill, M. R.; Lashewycz, R. A.; Rotella, F. J. *Inorg. Chem.* **1977**, *16*, 265.
(27) UCLA Crystallographic Computing Package, University of California, Los Angeles, 1981. Strouse, C. Personal communication.
(28) Nicolet Instrument Corp., Madison, WI, 1987.
(29) *International Tables for X-Ray Crystallography*; Kynoch Press: Birmingham, England, 1974: (a) pp 99–101; (b) pp 149–150.
(30) (a) Leising, R. A.; Grzybowski, J. J.; Takeuchi, K. J. *Inorg. Chem.* **1988**, *27*, 1020–1025 and references contained therein. (b) Sullivan, B. P.; Calvert, J. M.; Meyer, T. J. *Inorg. Chem.* **1980**, *19*, 1404–1407.

Scheme I

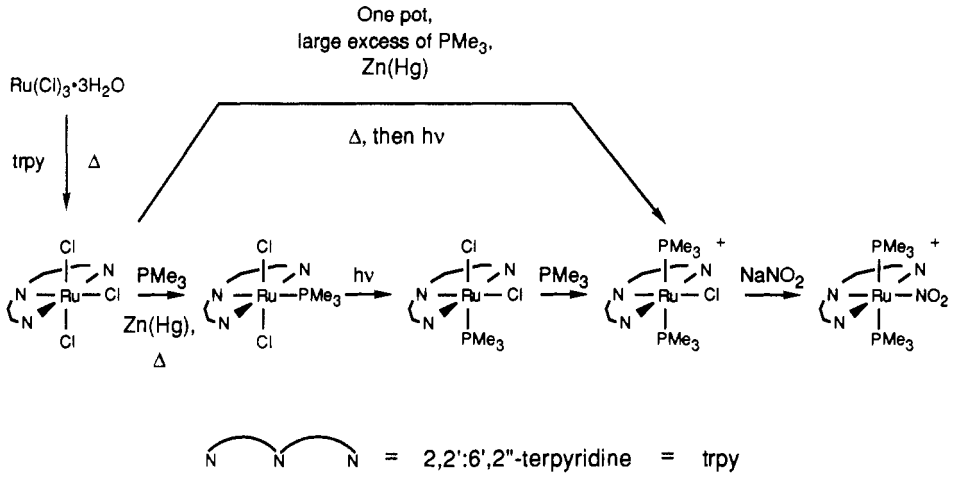

perchlorate salt, should only be handled in small quantities.[31]

***trans*-[RuCl(PMe$_3$)$_2$(trpy)](ClO$_4$).** A 0.060-g (0.125-mmol) sample of *cis*-[RuCl$_2$(PMe$_3$)(trpy)] was dissolved in a 30 mL solution of 2:1 acetone/ethanol (v/v). Then 1.5 equiv (0.014 g, 0.188 mmol) of PMe$_3$ was added to the solution, and the reaction was allowed to stir at room temperature for 3 h under an argon atmosphere. Then the solvent was completely removed with a rotary evaporator, and the solid residue was dissolved in 15 mL of H_2O. One gram of NaClO$_4$ was dissolved in 2 mL of H_2O, and this solution was added to the ruthenium solution to precipitate the product. The microcrystalline red-brown product was collected by vacuum filtration and washed with H_2O and Et_2O. Analytically pure *trans*-[RuCl(PMe$_3$)$_2$(trpy)](ClO$_4$) was obtained by eluting a solution of the microcrystalline material through an activated alumina column, using acetone as the eluent. The eluant was combined with an equal volume of toluene, and the acetone was removed with a rotary evaporator. The removal of the acetone resulted in the formation of microcrystalline analytically pure *trans*-[RuCl(PMe$_3$)$_2$(trpy)](ClO$_4$), which was collected by vacuum filtration and air-dried. A total of 0.061 g of product was isolated (yield 79%), and the yield starting from RuCl$_3$(trpy) was 34%. Anal. Calcd for $C_{21}H_{29}Cl_2N_3O_4P_2Ru \cdot 0.25C_6H_5CH_3$: C, 42.40; H, 4.85. Found: C, 42.60; H, 4.78.

***trans*-[Ru(NO$_2$)(PMe$_3$)$_2$(trpy)](ClO$_4$).** A 0.100-g (0.161-mmol) sample of *trans*-[RuCl(PMe$_3$)$_2$(trpy)](ClO$_4$) was added to 50 mL of a 1:1 H_2O/EtOH (v/v) solution containing 20 equiv of NaNO$_2$ (0.222 g, 3.220 mmol). The mixture was heated at reflux under N_2 for 3 h. After this time the solution was allowed to cool, then excess NaClO$_4$ (2.0 g in 20 mL of H_2O) was added, and the volume was slowly reduced through the use of a rotary evaporator. The product, *trans*-[Ru(NO$_2$)(PMe$_3$)$_2$(trpy)](ClO$_4$), precipitated out and was collected by vacuum filtration. The complex was purified by elution through an activated Al_2O_3 column, initially using a 1:1 acetonitrile/toluene (v/v) eluent, and then switching to a 3:1 acetonitrile/toluene (v/v) eluent, with collection of the red-orange band. The acetonitrile was slowly removed from the eluant with a rotary evaporator and the purified product precipitated as a red crystalline material. A total of 0.088 g (0.139 mmol) was isolated; yield 86%. Anal. Calcd for $C_{21}H_{29}ClN_4O_6P_2Ru$: C, 39.91; H, 4.62. found: C, 39.90; H, 4.62. The crystal of *trans*-[Ru^{II}(NO$_2$)(PMe$_3$)$_2$(trpy)](ClO$_4$) used for the structural determination was grown over a period of days, from a mixture of acetone and toluene.

Alternate Synthesis of *trans*-[RuCl(PMe$_3$)$_2$(trpy)](ClO$_4$). A 0.204-g (0.462-mmol) sample of RuCl$_3$(trpy) was added to 60 mL of N_2-outgassed CH_2Cl_2. Five equivalents of PMe$_3$ (2.310 mmol, 0.175 g) and 5 g of Zn(Hg) were added to the solution. The solution was heated at reflux for 8 h, during which time the color changed to dark blue-violet. The solution was then irradiated with a 120-W tungsten light for 12 h, during which time the color changed from blue-violet to red-brown. The solution was allowed to cool and then was filtered, and the solvent was completely removed with a rotary evaporator. The product was dissolved in 60 mL of a 3:1 H_2O/EtOH (v/v) solution, and excess aqueous NaClO$_4$ (2.0 g in 2 mL of H_2O) was added to the solution. The EtOH was removed slowly by use of a rotary evaporator, whereupon a microcrystalline solid precipitated out of solution. The red-brown precipitate was collected by vacuum filtration and washed with H_2O and Et_2O. A total of 0.257 g (0.414 mmol) of pure product was obtained; the yield starting with RuCl$_3$(trpy) was 90%. Anal. Calcd for $C_{21}H_{29}Cl_2N_3O_4P_2Ru \cdot 2H_2O$: C, 38.37; H, 5.06. Found: C, 38.01; H, 4.66.

***trans*-[Ru(^{15}NO$_2$)(PMe$_3$)$_2$(trpy)](ClO$_4$).** A 0.151-g (0.243-mmol) sample of *trans*-[RuCl(PMe$_3$)$_2$(trpy)](ClO$_4$) and 0.052 g (3 equiv, 0.742 mmol) of Na^{15}NO$_2$ were combined in 45 mL of a 1:1 H_2O/EtOH (v/v) solution. The solution was heated at reflux under N_2 for 4 h. The microcrystalline product was isolated by following the procedure for *trans*-[Ru(NO$_2$)(PMe$_3$)$_2$(trpy)](ClO$_4$). A total of 0.115 g (0.162 mmol) was obtained yield 67%.

Table I. Conductivity Data for *trans*-[RuCl(PMe$_3$)$_2$(trpy)](ClO$_4$) and *trans*-[Ru(NO$_2$)(PMe$_3$)$_2$(trpy)](ClO$_4$) in Acetonitrile and $E_{1/2}$ Potentials and ΔE_p Values for *trans*-[RuCl$_2$(PMe$_3$)(trpy)], *cis*-[RuCl$_2$(PMe$_3$)(trpy)], *trans*-[RuCl(PMe$_3$)$_2$(trpy)](ClO$_4$), and *trans*-[Ru(NO$_2$)(PMe$_3$)$_2$(trpy)](ClO$_4$)

(a) Conductivity Data

complex	Λ_0	B	electrolyte
trans-[RuCl(PMe$_3$)$_2$(trpy)](ClO$_4$)	137.8	253.6	1:1
trans-[Ru(NO$_2$)(PMe$_3$)$_2$(trpy)](ClO$_4$)	146.9	266.2	1:1

(b) Electrochemical Data

	$E_{1/2}$, V vs SSCE[a]	ΔE_p, V
trans-[RuCl$_2$(PMe$_3$)(trpy)]$^{+/0}$ [b]	+0.41	0.18
cis-[RuCl$_2$(PMe$_3$)(trpy)]$^{+/0}$ [b]	+0.57	0.10
trans-[RuCl(PMe$_3$)$_2$(trpy)]$^{2+/+}$ [c]	+0.73	0.07
trans-[Ru(NO$_2$)(PMe$_3$)$_2$(trpy)]$^{2+/+}$ [c]	+1.04	0.07

[a] $i_{p,c}/i_{p,a}$ = peak current ratio = 1.0 in all cases. [b] Conditions: 0.1 M Bu_4NBF_4 in CH_2Cl_2; Pt working electrode; SSCE reference electrode; scan rate 100 mV/s. [c] Conditions: 0.1 M TEAP in CH_3CN; Pt working electrode; SSCE reference electrode; scan rate 100 mV/s.

Results and Discussion

Synthesis and Analytical Data. This paper describes the complete five-step synthetic method outlined in our initial report.[21] The reactions for the formation of *trans*-[Ru(NO$_2$)(PMe$_3$)$_2$(trpy)](ClO$_4$) from RuCl$_3$·3H$_2$O are depicted in Scheme I. For the five-step synthesis, the overall yield for *trans*-[Ru(NO$_2$)(PMe)$_2$(trpy)](ClO$_4$) from RuCl$_3$·3H$_2$O is 27%.

The three-step synthesis utilizes the first reported one-pot method for the incorporation of trans-trimethylphosphine ligands into the coordination sphere of ruthenium, with an overall yield for *trans*-[Ru(NO$_2$)(PMe$_3$)$_2$(trpy)](ClO$_4$) from RuCl$_3$·3H$_2$O of 71%. While the second method resulted in much higher yields than the first method, the first method is more flexible, where two different phosphine ligands can be added to the ruthenium center.[70]

Conductivity Data. Conductivity measurements were performed on both *trans*-[RuCl(PMe$_3$)$_2$(trpy)](ClO$_4$) and *trans*-[Ru(NO$_2$)(PMe$_3$)$_2$(trpy)](ClO$_4$). The measurements were conducted by applying the method of Feltham and Hayter,[25] using five stock solutions of different concentrations for both *trans*-[RuCl(PMe$_3$)$_2$(trpy)](ClO$_4$) and *trans*-[Ru(NO$_2$)(PMe$_3$)$_2$(trpy)](ClO$_4$), in the range of 1.5–15 mM. The conductivities of the two com-

(31) (a) Wolsey, W. C. *J. Chem. Educ.* **1973**, *50*, A335–A337. (b) Raymond, K. *Chem. Eng. News* **1983**, *61* (Dec 5), 4.

plexes are listed in Table Ia, and these values were consistent with 1:1 monomeric salts, when compared directly to literature values for transition metal complexes containing perchlorate anions in acetonitrile.[30a,32] The data are given in the form of Λ_0, which is the conductance at infinite dilution, and B, the slope of a plot of $\Lambda_0 - \Lambda_e$ against the square root of c (where c is the equivalent concentration of the compound being measured and Λ_e is the observed conductivity).

Cyclic Voltammetry. Cyclic voltammetry was conducted on *cis*- and *trans*-$[RuCl_2(PMe_3)(trpy)]$, with the data listed in Table Ib. These complexes displayed one reversible $[RuCl_2(PMe_3)(trpy)]^{+/0}$ couple. This one-electron-oxidation process is chemically and electrochemically reversible, as evidenced by peak current ratios ($i_{p,a}/i_{p,c} = 1.0$) and by peak potential separations consistent with that of the ferrocene couple when it is measured under identical conditions.

In addition, cyclic voltammetry was conducted on *trans*-$[RuCl(PMe_3)_2(trpy)](ClO_4)$ and *trans*-$[Ru(NO_2)(PMe_3)_2(trpy)](ClO_4)$, with the data listed in Table Ib. The cyclic voltammogram for *trans*-$[Ru(NO_2)(PMe_3)_2(trpy)](ClO_4)$ displayed one reversible $[Ru(NO_2)(PMe_3)_2(trpy)]^{2+/+}$ couple, as evidenced by peak current ratios ($i_{p,a}/i_{p,c} = 1.0$) and by peak potential separations of 60–70 mV. Plots of the peak currents versus the square root of scan velocity at scan rates from 50 to 400 mV/s are linear, which implies diffusion-controlled reversibility, by the Randles–Sevcik equation.[33]

The $[Ru(NO_2)(PMe_3)_2(trpy)]^{2+/+}$ couple for *trans*-$[Ru(NO_2)(PMe_3)_2(trpy)](ClO_4)$ is reversible, unlike the (nitro)ruthenium(II) complex $[Ru(bpy)_2(Cl)(NO_2)]^+$.[34a] The cyclic voltammetry of $[Ru(bpy)_2(Cl)(NO_2)]^+$ showed that the one-electron oxidation was followed by rapid disproportionation of the oxidized species, producing the corresponding (nitrosyl)ruthenium(II) and (nitrato)ruthenium(III) complexes. The stabilization of the electrochemically generated (nitro)ruthenium(III) complex from *trans*-$[Ru(NO_2)(PMe_3)_2(trpy)](ClO_4)$ has been achieved through the utilization of trans-trimethylphosphine ligands, in combination with a 2,2′:6′,2″-terpyridine ligand, where cyclic voltammetry demonstrates that rapid disproportionation does not occur with *trans*-$[Ru(NO_2)(PMe_3)_2(trpy)](ClO_4)$.

Coulometry. Controlled-potential electrolysis was carried out on the *trans*-$[Ru(NO_2)(PMe_3)_2(trpy)](ClO_4)$ complex in acetonitrile solution, and the product was monitored by cyclic voltammetry. Exhaustive electrolysis past the oxidative wave of the Ru(III)/Ru(II) couple (the potential was held at +1.40 V vs SSCE) gave a value of $n = 1.1$, and the cyclic voltammogram of the solution was consistent with the quantitative conversion to *trans*-$[Ru(NO_2)(PMe_3)_2(trpy)]^{2+}$.[21] Then, exhaustive electrolysis for the return reduction of the species gave an $n = 1.0$ value, showing that *trans*-$[Ru(NO_2)(PMe_3)_2(trpy)]^+$ re-forms quantitatively.

IR Spectra. The IR spectrum of *trans*-$[Ru(NO_2)(PMe_3)_2(trpy)](ClO_4)$ was used to investigate the bonding mode of the nitro ligand. Assignments of the ν_{as} (asymmetric stretch) and ν_s (symmetric stretch) bands were made on the basis of a careful peak by peak comparison of the spectra of *trans*-$[Ru(NO_2)(PMe_3)_2(trpy)](ClO_4)$ with the spectra of *trans*-$[RuCl(PMe_3)_2(trpy)](ClO_4)$. Confirmation of the assignment was accomplished through a $^{15}NO_2$ isotopic labeling study on *trans*-$[Ru(NO_2)(PMe_3)_2(trpy)](ClO_4)$ (see Figure 1a,b). The results of these studies are listed in Table IIa.

The ν_{as} band for *trans*-$[Ru(NO_2)(PMe_3)_2(trpy)](ClO_4)$ shifted to lower frequencies when the ligand was changed from $^{14}NO_2$ to $^{15}NO_2$. The shift of 29 cm^{-1} is 121% of the calculated shift based on a Hooke's law approximation (shifts of larger than 100% have often been observed for other NO_2 labeling studies, due to the inability of Hooke's law to account for the more complicated NO_2 vibrations).[35] The corresponding ν_s band also shifted to lower frequencies by 22 cm^{-1}, which is 96% of the calculated shift based on Hooke's law. These frequencies and shifts are consistent with other N-bound NO_2 complexes,[35-37] including the observations for the $[Ru(bpy)_2Cl(NO_2)]^{2+}$ complex, where greater than 100% of the calculated shift, based on a Hooke's law approximation, was observed for both ν_{as} and ν_s bands.[34b] The N-bound NO_2 coordination of the *trans*-$[Ru(NO_2)(PMe_3)_2(trpy)](ClO_4)$ has also been confirmed by the X-ray structural determination and analysis.

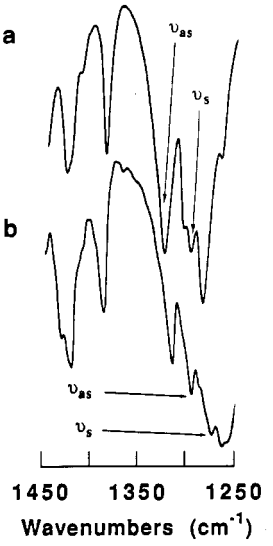

Figure 1. Portion of IR spectra for (a) *trans*-$[Ru(NO_2)(PMe_3)_2(trpy)](ClO_4)$, and (b) *trans*-$[Ru(^{15}NO_2)(PMe_3)_2(trpy)](ClO_4)$. Arrows denote bands corresponding to N–O stretches.

Table II. Infrared Spectroscopic Data for the ν_{N-O} Bands of *trans*-$[Ru(NO_2)(PMe_3)_2(trpy)](ClO_4)$ and UV–Visible Spectral Data for *trans*-$[RuCl_2(PMe_3)(trpy)]$, *cis*-$[RuCl_2(PMe_3)(trpy)]$, *trans*-$[RuCl(PMe_3)_2(trpy)](ClO_4)$, and *trans*-$[Ru(NO_2)(PMe_3)_2(trpy)](ClO_4)$

(a) Infrared Data

complex	ν_{as}, cm^{-1} [a]	ν_s, cm^{-1} [b]
trans-$[Ru(NO_2)(PMe_3)_2(trpy)](ClO_4)$	1324	1297
trans-$[Ru(^{15}NO_2)(PMe_3)_2(trpy)](ClO_4)$	1295	1275

(b) UV–Visible Data

complex	λ_{max}, nm ($10^{-3}\epsilon$, M^{-1} cm^{-1})
trans-$[RuCl_2(PMe_3)(trpy)]$ [c]	636 (sh),[f] 562 (4.0),[e] 409 (4.5),[e] 330 (7.6), 317 (15.3), 284 (13.5)
cis-$[RuCl_2(PMe_3)(trpy)]$ [c]	554 (4.0),[e] 498 (sh),[f] 370 (4.2),[e] 319 (21.4), 273 (17.1)
trans-$[RuCl(PMe_3)_2(trpy)](ClO_4)$ [d]	494 (4.5),[e] 451 (sh),[f] 346 (sh),[f] 308 (32.0), 271 (20.2)
trans-$[Ru(NO_2)(PMe_3)_2(trpy)](ClO_4)$ [d]	450 (sh),[f] 430 (4.9),[e] 308 (29.9), 272 (18.0)

[a] ν_{as} = the asymmetric NO_2 stretching mode. [b] ν_s = the symmetric NO_2 stretching mode. [c] Spectrum recorded in CH_2Cl_2. [d] Spectrum recorded in CH_3CN. [e] Very broad absorbance. [f] sh = shoulder.

Electronic Absorption Spectra. The spectral data for all complexes are contained in Table IIb. For *trans*-$[RuCl_2(PMe_3)(trpy)]$, the transitions at 636, 562, and 409 nm are primarily due to

(32) Davies, J. A.; Hartley, F. R.; Murray, S. G. *Inorg. Chim. Acta* **1980**, *43*, 69–72.
(33) Brown, E. R.; Large, R. F. *Physical Methods of Chemistry*; Wiley-Interscience: New York, 1971; Vol. 1, Part IIA, Chapter 6.
(34) (a) Keene, F. R.; Salmon, D. J.; Walsh, J. L.; Abruna, H. D.; Meyer, T. J. *J. Am. Chem. Soc.* **1980**, *19*, 1896–1903. (b) Nagao, H.; Mukaida, M.; Shimizu, K.; Howell, F. S.; Kakihana, H. *Inorg. Chem.* **1986**, *25*, 4312–4314.
(35) (a) Cleare, M. J.; Griffith, W. P. *J. Chem. Soc. A* **1967**, 1144–1147. (b) Pinchase, S.; Lauchlit, I. *Infrared Spectra of Labelled Compounds*; Academic Press: London, 1971.
(36) Nakamoto, K. *Infrared and Raman Spectra of Inorganic and Coordination Compounds*, 4th ed.; Wiley: New York, 1986.
(37) Adeymi, S. A.; Miller, F. J.; Meyer, T. J. *Inorg. Chem.* **1972**, *11*, 994–999.

Table III. ^{1}H NMR Spectral Data and Proton-Decoupled ^{13}C NMR Spectral Data for *trans*-[RuCl(PMe$_3$)$_2$(trpy)](ClO$_4$) and *trans*-[Ru(NO$_2$)(PMe$_3$)$_2$(trpy)](ClO$_4$) in CDCl$_3$

(a) ^{1}H NMR Data

complex	δ^a (multiplicity) [J, Hz] {assignment};^{c} phosphine	trpy
trans-[RuCl(PMe$_3$)$_2$(trpy)](ClO$_4$)	0.7 (T, 18 H) [3.4] {CH$_3$–}	7.6 (t, 2 H) [6.5] {H(5,5″)}, 8.1 (t, 3 H) [7.8] {H(4,4′,4″)}, 8.6 (d, 4 H) [7.8] {H(3,3′,3″,5′)}, 9.0 (d, 2 H) [5.8] {H(6,6″)}
trans-[Ru(NO$_2$)(PMe$_3$)$_2$(trpy)](ClO$_4$)	0.7 (T, 18 H) [3.5] {CH$_3$–}	7.7 (t, 2 H) [6.6] {H(5,5″)}, 8.2 (t, 3 H) [7.8] {H(4,4′,4″)}, 8.6 (d, 4 H) [7.9] {H(3,3′,3″,5′)}, 9.7 (d, 2 H) [5.6] {H(6,6″)}

(b) ^{13}C NMR Data

	δ^b (multiplicity) [J, Hz]^c	
	phosphine	trpy
trans-[RuCl(PMe$_3$)$_2$(trpy)](ClO$_4$)	9.7 (T) [13.9] {CH$_3$–}	123.2, 123.9, 127.2, 132.1, 136.8, 152.3, 157.2, 157.7
trans-[Ru(NO$_2$)(PMe$_3$)$_2$(trpy)](ClO$_4$)	10.0 (T) [13.4] {CH$_3$–}	122.8, 124.0, 126.9, 135.8, 137.4, 153.4, 155.4, 156.6

^{a} All shifts are relative to Me$_4$Si internal standard. ^{b} Chemical shift is relative to the center line of CDCl$_3$ (77.00). ^{c} All absorbances are singlets unless otherwise noted. Abbreviations used: d = doublet ($J = {}^3J_{HH}$); t = triplet ($J = {}^3J_{HH}$); q = quartet ($J = {}^3J_{HH}$); m = multiplet; T = second-order virtually coupled, 1:2:1 triplet.

Ru(dπ) → (trpy)π^* metal-to-ligand charge transfers (MLCT) as observed for other trans-(phosphine)ruthenium(II) complexes.[30a,38-41] The transitions observed at 330, 317, and 284 nm have been assigned as $\pi \rightarrow \pi^*$(trpy) ligand-localized transitions, in analogy to those for other reported (terpyridine)ruthenium complexes.[38-42]

The conversion of *trans*- to *cis*-[RuCl$_2$(PMe$_3$)(trpy)] is characterized by a shift to shorter wavelengths for two of the MLCT transitions. The transition at 636 nm shifts to 498 nm, while the transition at 410 nm shifts to 370 nm. The remaining MLCT transition is unchanged by the interconversion. The two ligand-localized $\pi \rightarrow \pi^*$(trpy) transitions remain essentially unchanged, occurring at 321 and 275 nm.

The addition of the second phosphine to the *cis*-[RuCl$_2$(PMe$_3$)(trpy)] complex and the change from a neutral to a positively charged complex result in a shift of all of the MLCT transitions to shorter wavelengths. The spectral data from *trans*-[RuCl(PMe$_3$)$_2$(trpy)](ClO$_4$) and *trans*-[Ru(NO$_2$)(PMe$_3$)$_2$(trpy)](ClO$_4$) are presented in Table IIb. The observed spectral characteristics are consistent with the spectra of other (terpyridine)ruthenium(II) complexes.[30a,38-45] For *trans*-[RuCl(PMe$_3$)$_2$(trpy)](ClO$_4$), the transitions at 494, 451, and 346 nm are primarily Ru(dπ) → (trpy)π^* metal-to-ligand charge transfer (MLCT) as observed for other (terpyridine)ruthenium(II) complexes.[30a,38-41] The transitions observed at 308 and 271 nm have been assigned as $\pi \rightarrow \pi^*$(trpy) ligand localized transitions, in analogy to those of similar (terpyridine)ruthenium complexes.[38-42]

The spectral features of the *trans*-[Ru(NO$_2$)(PMe$_3$)$_2$(trpy)](ClO$_4$) complex (see Figure 2) contain three primary absorbances between 750 and 250 nm. Two MLCT bands appear to overlap, occurring at 450 and 430 nm, respectively, decreasing the distinction between the two transitions. The shifts to shorter wavelengths are consistent with the observed increase in the potential of the [Ru(NO$_2$)(PMe$_3$)$_2$(trpy)]$^{2+/+}$ couple, relative to the potential for the [RuCl(PMe$_3$)$_2$(trpy)]$^{2+/+}$ couple. Similar trends have been reported in the literature for other (polypyridyl)ruthenium(II) complexes, where the increase in the $E_{1/2}$ for the complex is accompanied by a shift to shorter wavelengths for the lowest energy MLCT transition.[46] The region between 250 and 350 nm is still dominated by the two ligand localized $\pi \rightarrow \pi^*$(trpy) transitions.

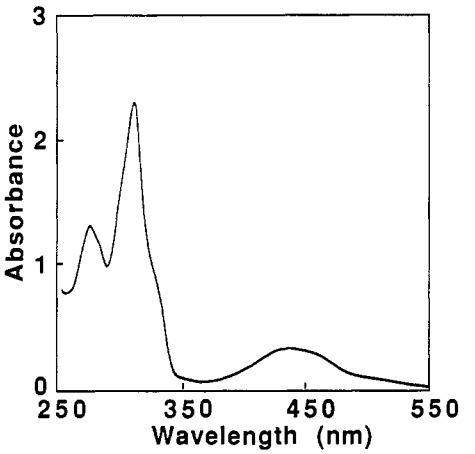

Figure 2. Electronic spectrum of *trans*-[Ru(NO$_2$)(PMe$_3$)$_2$(trpy)](ClO$_4$) (5.70×10^{-5} M) in CH$_3$CN.

NMR Spectra. ^{1}H and ^{13}C NMR spectroscopies were utilized to determine the ligand arrangement about the ruthenium center for both *trans*-[RuCl(PMe$_3$)$_2$(trpy)](ClO$_4$) and *trans*-[Ru(NO$_2$)(PMe$_3$)$_2$(trpy)](ClO$_4$). The results of these studies are contained in Table III (part a, ^{1}H data, and part b, ^{13}C data). Both complexes displayed spectra that are consistent with their formulations.

The observed chemical shifts and splitting patterns for the respective trpy rsonances were similiar for both *trans*-[Ru(NO$_2$)(PMe$_3$)$_2$(trpy)](ClO$_4$) and *trans*-[RuCl(PMe$_3$)$_2$(trpy)](ClO$_4$), and the data collected for these species were consistent with the data for both the free trpy ligand[47] and for a standard (trpy)Ru^{II} complex: [Ru(trpy)$_2$](PF$_6$)$_2$.[48] The splitting patterns observed for the trpy resonances on the both *trans*-[RuCl(PMe$_3$)$_2$(trpy)](ClO$_4$) and *trans*-[Ru(NO$_2$)(PMe$_3$)$_2$(trpy)](ClO$_4$) suggest an overall C_{2v} symmetry for the complexes, which was confirmed by the crystal structure of *trans*-[Ru(NO$_2$)(PMe$_3$)$_2$(trpy)](ClO$_4$). The assignments of the shifts (see Table IIIa) were based on the assignments reported for the ^{1}H NMR spectrum of the free ligand,[47] and for other terpyridine complexes, including bis(terpyridine)ruthenium(II).[48-51] The chemical shifts of the protons in the H(6,6″) positions on the terpyridine were sensitive to the nature of the adjacent ligand (chloro or nitro), where the H(6,6″) signal occurs at δ 9.0 for *trans*-[RuCl(PMe$_3$)$_2$(trpy)](ClO$_4$) while for *trans*-[Ru(NO$_2$)(PMe$_3$)$_2$(trpy)](ClO$_4$) it appears

(38) Thummel, R. P.; Jahng, Y. *Inorg. Chem.* **1986**, *25*, 2527–2534.
(39) Calvert, J. M.; Peebles, D. L.; Nowak, R. J. *Inorg. Chem.* **1985**, *24*, 3111–3119.
(40) Calvert, J. M.; Meyer, T. J. *Inorg. Chem.* **1985**, *20*, 27–33.
(41) Root, M. J.; Deutsch, E. *Inorg. Chem.* **1985**, *24*, 1464–1471.
(42) Suen, H. F.; Wilson, S. W.; Pomerantz, M.; Walsh, J. L. *Inorg. Chem.* **1989**, *28*, 786–791.
(43) Berger, R. M.; McMillan, D. R. *Inorg. Chem.* **1988**, *27*, 4245–4249.
(44) Kroener, R.; Heeg, M. J.; Deutsch, E. *Inorg. Chem.* **1988**, *27*, 558–566.
(45) Neyhart, G. A.; Meyer, T. J. *Inorg. Chem.* **1986**, *25*, 4807–4808.
(46) Dodsworth, E. S.; Lever, A. B. P. *Chem. Phys. Lett.* **1985**, *119*, 61–66.
(47) Constable, E. C. *J. Chem. Soc., Dalton Trans.* **1985**, 2687–2689.
(48) Lytle, F. E.; Petrosky, L. M.; Carlson, L. R. *Anal. Chim. Acta* **1971**, *57*, 239–247.
(49) Castellano, S.; Gunther, H.; Ebersole, S. *J. Phys. Chem.* **1965**, *69*, 4166.
(50) Orellana, G.; Ibarra, C. A.; Santoro, J. *Inorg. Chem.* **1988**, *27*, 1025–1030.
(51) Seok, W. K.; Meyer, T. J. *J. Am. Chem. Soc.* **1988**, *110*, 7358–7367.

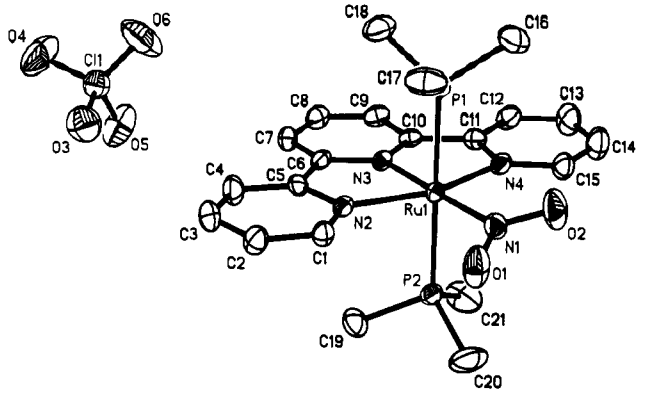

Figure 3. Labeling diagram for *trans*-[Ru(NO2)(PMe3)2(trpy)](ClO4) (ORTEP diagram; hydrogen atoms omitted).

Table IV. Experimental Data for X-ray Diffraction Study of [Ru(NO2)(PMe3)2(trpy)](ClO4)

formula: $C_{21}H_{29}ClN_4O_6P_2Ru$
fw: 631.9
cryst syst: monoclinic
space group: $P2_1/c$ (C_{2h}^5; No. 14)
a = 16.102 (11) Å
b = 10.365 (7) Å
c = 16.788 (12) Å
β = 108.23 (5)°
V = 2661 (3) Å^3
Z = 4
D_{calcd}, g/cm^3 = 1.58
diffractometer: Syntex $P2_1$
radiation: Mo Kα ($\bar{\lambda}$ = 0.710 730 Å)
monochromator: highly oriented graphite; equatorial mode
data collected: $+h,+k,\pm l$
scan type: coupled θ(crystal)–2θ(counter)
scan width: sym [$2\theta(K\alpha_1) - 1.0$] → [$2\theta(K\alpha_2) + 1.0$]
scan speed: 4.0 deg min^{-1} (in 2θ)
$2\theta_{max}$, deg: 45.0
μ(Mo Kα), cm^{-1} = 8.38
tot. no. of reflcns collcd: 3902
no. of unique reflcns: 3169 ($F_o > 0$)
no. of variables: 316
R_F = 7.1%
R_wF = 6.4%
goodness of fit: 1.01

at δ 9.8. This change is most likely caused by the increased deshielding of the more electron-withdrawing nitro group.

The resonance for the methyl protons of the trans-trimethylphosphine ligands in both *trans*-[RuCl(PMe3)2(trpy)](ClO4) and *trans*-[Ru(NO2)(PMe3)2(trpy)](ClO4) occurs at 0.7 ppm in the ^{1}H NMR spectrum, and both are split into a 1:2:1 triplet, due to the virtual coupling of the trans phosphorus atoms, where the coupling constant, J, is equal to 3.5 Hz. The appearance of a virtually coupled triplet for the methyl protons of the bis(trimethylphosphine)ruthenium(II) complex strongly suggests a trans arrangement of the phosphine ligands,[52-57] which was also corroborated by the X-ray crystal structure.

The completely proton-decoupled ^{13}C NMR spectra for both *trans*-[RuCl(PMe3)2(trpy)](ClO4) and *trans*-[Ru(NO2)(PMe3)2(trpy)](ClO4) also suggest an overall C_{2v} symmetry for both complexes, consistent with an octahedral, trans-phosphine configuration. The spectra for these complexes, display nine resonances, eight of which (123–157 ppm) are due to the eight unique carbon atoms of the planar 2,2′:6′,2″-terpyridine ligand. The remaining resonance at 10 ppm, is due to the six chemically equivalent carbon atoms from the two phosphine ligands. This resonance is split into a virtual triplet due to coupling with both phosphorus nuclei, with J = 13 Hz. This also indicates a trans arrangement of the phosphine ligands.[58]

Crystal Structure of [Ru(NO2)(PMe3)2(trpy)](ClO4). The crystal consists of an array of [Ru(NO2)(PMe3)2(trpy)]$^+$ cations and [ClO4]$^-$ anions in a 1:1 stoichiometry. Atomic coordinates and equivalent isotropic displacement parameters are given in

Table V. Atomic Coordinates (×10^4) and Equivalent Isotropic Displacement Parameters (Å^2 × 10^3)

atom	x	y	z	U(eq)[a]
Ru(1)	3174.2 (4)	1550.2 (6)	1407.0 (3)	29.1 (2)
P(1)	2279 (1)	704 (2)	2158 (1)	37 (1)
P(2)	4124 (1)	2326 (2)	686 (1)	41 (1)
N(1)	4215 (4)	1349 (7)	2501 (4)	44 (3)
N(2)	3177 (4)	−264 (6)	868 (3)	34 (2)
N(3)	2151 (4)	1715 (6)	379 (3)	32 (2)
N(4)	2745 (4)	3413 (6)	1558 (4)	40 (2)
O(1)	4800 (4)	525 (7)	2589 (4)	82 (3)
O(2)	4295 (4)	2029 (8)	3111 (4)	88 (3)
C(1)	3732 (5)	−1258 (7)	1148 (4)	37 (3)
C(2)	3651 (5)	−2416 (8)	736 (5)	49 (4)
C(3)	2974 (6)	−2599 (9)	6 (6)	58 (4)
C(4)	2404 (6)	−1573 (9)	−309 (5)	54 (3)
C(5)	2503 (5)	−420 (8)	126 (4)	37 (3)
C(6)	1918 (5)	687 (8)	−153 (4)	36 (3)
C(7)	1202 (5)	765 (8)	−871 (5)	42 (3)
C(8)	715 (5)	1906 (9)	−1013 (5)	48 (3)
C(9)	936 (5)	2934 (9)	−453 (5)	46 (3)
C(10)	1678 (5)	2821 (8)	252 (5)	34 (3)
C(11)	2008 (5)	3773 (7)	922 (5)	39 (3)
C(12)	1600 (6)	4970 (8)	927 (6)	55 (4)
C(13)	1955 (7)	5775 (9)	1599 (7)	70 (5)
C(14)	2695 (6)	5436 (10)	2228 (6)	73 (5)
C(15)	3079 (6)	4254 (8)	2183 (5)	51 (4)
C(16)	2019 (7)	1773 (10)	2886 (6)	77 (5)
C(17)	2731 (6)	−684 (9)	2784 (6)	71 (5)
C(18)	1208 (6)	147 (10)	1540 (5)	71 (4)
C(19)	4074 (6)	1426 (9)	−255 (5)	61 (4)
C(20)	5256 (6)	2313 (16)	1239 (6)	121 (7)
C(21)	3920 (8)	3973 (10)	285 (8)	98 (6)
Cl (1)	453 (1)	−3513 (3)	−1482 (1)	57 (1)
O(3)	1242 (5)	−4216 (7)	−1137 (5)	87 (4)
O(4)	−181 (5)	−4332 (9)	−2021 (5)	121 (4)
O(5)	641 (5)	−2486 (7)	−1960 (4)	97 (4)
O(6)	203 (6)	−3072 (11)	−813 (5)	136 (5)

[a] Equivalent isotropic U defined as one-third of the trace of the orthogonalized U_{ij} tensor.

Table VI. Interatomic Distances (Å) with Esd's

Ru(1)–P(1)	2.361 (3)	Ru(1)–P(2)	2.368 (3)
Ru(1)–N(1)	2.074 (6)	Ru(1)–N(2)	2.088 (6)
Ru(1)–N(3)	1.985 (5)	Ru(1)–N(4)	2.093 (7)
P(1)–C(16)	1.794 (11)	P(1)–C(17)	1.796 (10)
P(1)–C(18)	1.806 (8)	P(2)–C(19)	1.815 (9)
P(2)–C(20)	1.769 (9)	P(2)–C(21)	1.826 (11)
N(1)–O(1)	1.245 (10)	N(1)–O(2)	1.217 (10)
N(2)–C(1)	1.348 (9)	N(2)–C(5)	1.382 (8)
N(3)–C(6)	1.365 (9)	N(3)–C(10)	1.356 (10)
N(4)–C(11)	1.377 (9)	N(4)–C(15)	1.341 (10)
C(1)–C(2)	1.371 (11)	C(2)–C(3)	1.375 (11)
C(3)–C(4)	1.396 (12)	C(4)–C(5)	1.383 (12)
C(5)–C(6)	1.465 (11)	C(6)–C(7)	1.386 (9)
C(7)–C(8)	1.398 (12)	C(8)–C(9)	1.391 (12)
C(9)–C(10)	1.400 (9)	C(10)–C(11)	1.464 (10)
C(11)–C(12)	1.404 (12)	C(12)–C(13)	1.376 (13)
C(13)–C(14)	1.368 (13)	C(14)–C(15)	1.384 (14)
Cl(1)–O(3)	1.421 (7)	Cl(1)–O(4)	1.416 (8)
Cl(1)–O(5)	1.423 (8)	Cl(1)–O(6)	1.383 (11)

(52) Krassowski, D. W.; Nelson, J. H.; Brower, K. R.; Hauenstein, D.; Jacobson, R. A. *Inorg. Chem.* **1988**, *27*, 4294–4307.
(53) Harris, R. K. *Can. J. Chem.* **1964**, *42*, 2275–2281.
(54) Verkade, J. G. *Coord. Chem. Rev.* **1972/1973**, *9*, 1.
(55) Rosete, R. O.; Cole-Hamilton, D. J.; Wilkinson, G. *J. Chem. Soc., Dalton Trans.* **1984**, 2067.
(56) Probitts, E. J.; Saunders, D. R.; Stone, D. H.; Mawby, R. J. *J. Chem. Soc., Dalton Trans.* **1986**, 1167 and references therein.
(57) de C. T. Carrondo, M. A. A. F.; Rudolf, P. R.; Skapski, A. C.; Hornback, J. R.; Wilkinson, G. *Inorg. Chim. Acta* **1977**, *24*, L95.
(58) Axelson, D. E.; Holloway, C. E. *J. Chem. Soc., Chem. Commun.* **1973**, *36*, 325–355.

Table VII. Bond Angles (deg) with Esd's

P(1)-Ru(1)-P(2)	177.3 (1)	P(1)-Ru(1)-N(1)	87.1 (2)
P(2)-Ru(1)-N(1)	90.8 (2)	P(1)-Ru(1)-N(2)	88.9 (2)
P(2)-Ru(1)-N(1)	89.7 (2)	N(1)-Ru(1)-N(2)	100.5 (2)
P(1)-Ru(1)-N(3)	91.0 (2)	P(2)-Ru(1)-N(3)	91.1 (2)
N(1)-Ru(1)-N(3)	178.1 (3)	N(2)-Ru(1)-N(3)	79.3 (2)
P(1)-Ru(1)-N(4)	89.9 (2)	P(2)-Ru(1)-N(4)	92.2 (2)
N(1)-Ru(1)-N(4)	101.0 (3)	N(2)-Ru(1)-N(4)	158.3 (2)
N(3)-Ru(1)-N(4)	79.0 (2)	Ru(1)-P(1)-C(16)	116.5 (4)
Ru(1)-P(1)-C(17)	114.0 (4)	C(16)-P(1)-C(17)	103.6 (5)
Ru(1)-P(1)-C(18)	116.4 (3)	C(16)-P(1)-C(18)	101.8 (5)
C(17)-P(1)-C(18)	102.7 (4)	Ru(1)-P(2)-C(19)	114.2 (3)
Ru(1)-P(2)-C(20)	117.0 (4)	C(19)-P(2)-C(20)	102.1 (5)
Ru(1)-P(2)-C(21)	115.8 (5)	C(19)-P(2)-C(21)	101.9 (5)
C(20)-P(2)-C(21)	103.7 (6)	Ru(1)-N(1)-O(1)	123.1 (5)
Ru(1)-N(1)-O(2)	122.1 (6)	O(1)-N(1)-O(2)	114.8 (6)
Ru(1)-N(2)-C(1)	128.9 (4)	Ru(1)-N(2)-C(5)	112.9 (5)
C(1)-N(2)-C(5)	118.3 (6)	Ru(1)-N(3)-C(6)	119.0 (5)
Ru(1)-N(3)-C(10)	118.8 (4)	C(6)-N(3)-C(10)	122.1 (5)
Ru(1)-N(4)-C(11)	113.2 (5)	Ru(1)-N(4)-C(15)	128.9 (5)
C(11)-N(4)-C(15)	117.9 (7)	N(2)-C(1)-C(2)	123.0 (6)
C(1)-C(2)-C(3)	119.6 (7)	C(2)-C(3)-C(4)	118.4 (8)
C(3)-C(4)-C(5)	120.3 (7)	N(2)-C(5)-C(4)	120.3 (7)
N(2)-C(5)-C(6)	116.2 (7)	C(4)-C(5)-C(6)	123.5 (6)
N(3)-C(6)-C(5)	112.6 (5)	N(3)-C(6)-C(7)	120.5 (7)
C(5)-C(6)-C(7)	126.9 (7)	C(6)-C(7)-C(8)	117.8 (7)
C(7)-C(8)-C(9)	121.5 (6)	C(8)-C(9)-C(10)	118.5 (8)
N(3)-C(10)-C(9)	119.5 (7)	N(3)-C(10)-C(11)	113.5 (5)
C(9)-C(10)-C(11)	127.0 (7)	N(4)-C(11)-C(10)	115.5 (6)
N(4)-C(11)-C(12)	121.7 (7)	C(10)-C(11)-C(12)	122.8 (6)
C(11)-C(12)-C(13)	117.8 (7)	C(12)-C(13)-C(14)	121.0 (9)
C(13)-C(14)-C(15)	118.8 (9)	N(4)-C(15)-C(14)	122.8 (7)
O(3)-Cl(1)-O(4)	109.1 (5)	O(3)-Cl(1)-O(5)	107.0 (5)
O(4)-Cl(1)-O(5)	109.0 (5)	O(3)-Cl(1)-O(6)	106.8 (5)
O(4)-Cl(1)-O(6)	112.5 (6)	O(5)-Cl(1)-O(6)	112.3 (6)

Table V, interatomic distances and their estimated standard deviations are listed in Table VI, and bond angles with their esd's are listed in Table VII.

A perspective view and the numbering scheme for the molecule are shown in Figure 3. The results of the crystal structure confirm the C_{2v} geometry assigned to the complex. Among the noteworthy details offered by this structural determination is the coordination mode of the nitrite ligand. Nitrite is known to coordinate to a metal center in three different ways, ones as a nitrogen-bound nitro ligand and two as oxygen-bound coordination modes, as either a mono- or a bidentate nitrito ligand. All three of these coordination geometries have been confirmed through crystallographic studies.[59,60] The nitrite ligand in this complex is bound to the ruthenium center through the nitrogen atom, which is consistent with the ν_{N-O} bands found in the IR spectrum for this complex. The Ru-N(nitro) bond distance of 2.074 (6) Å found in this complex is very similiar to that reported for other (nitro)ruthenium(II) complexes, such as 2.078 (3), and 2.080 (3) Å for $Na_2[Ru(NO_2)_4(NO)(OH)]$.[61] The two N-O bond distances for the nitro ligand from our complex are 1.245 (10) and 1.217 (10) Å, and the O-N-O bond angle of 114.8 (6)° is on the lower end of the range for ∠O-N-O (113-127°) for transition-metal nitro complexes with cobalt, nickel, copper, palladium, platinum, and ruthenium.[59,62] The Ru-N-O angles are almost symmetrical, where the angles lie at 122.1 (6) and 123.1 (5)°. The nitro ligand is coordinated so that the O-N-O plane is tilted slightly out of the plane containing the 2,2′:6′,2″-terpyridine ligand. The Ru(trpy) moiety is essentially planar (rms deviation = 0.038 Å); N(1) is only 0.013 Å from the plane, and the NO_2 ligand makes an angle of 19.8° with that plane.

The trans arrangement of the phosphine ligands on $[Ru(NO_2)(PMe_3)_2(trpy)](ClO_4)$ was originally proposed from the ^{13}C and ^1H NMR data for this complex, and this was confirmed by the X-ray structural analysis. A significant body of crystallographic data has been assembled in the literature on (phosphine)ruthenium(II) complexes.[63] On this complex, the two trimethylphosphine ligands are almost directly in trans positions, as evidenced by the P-Ru-P bond angle of 177.3 (1)°. This value is close to that observed for other trans-(phosphine)ruthenium(II) complexes.[64-67] The Ru-P bond distances observed in this study are also almost identical, at 2.361 (3) and 2.368 (3) Å and fall within the range (2.26-2.41 Å) reported for other phosphine(ruthenium) complexes.[64-69]

The 2,2′:6′,2″-terpyridine ligand is bound to the three remaining coordination sites in a meridional fashion through the three nitrogen atoms of the pyridine rings. The central pyridine of the tridentate ligand is bound trans to the nitro ligand, with an observed N(nitro)-Ru-N(trpy) angle of 178.1 (3)°. The geometrical constraints of the trpy ligand cause a distinct, but symmetrical, variation from octahedral coordination. The pyridine rings on either end of the ligand bind to ruthenium at angles ∠N(2)-Ru-N(3) of 79.3 (2)° and ∠N(3)-Ru-N(4) of 79.0 (2)°, which show that trpy is constrained such that it cannot bind to ruthenium in an ideal (90°) geometry. The bond lengths for M-N(trpy) also confirm this observation, where the bond length for the center pyridine (Ru-N(3)) is 1.985 (5) Å and the bond distances for the two side pyridines are longer at 2.088 (6) and 2.093 (7) Å.

Acknowledgment. This work was supported in part by the donors of the Petroleum Research Fund, administered by the American Chemical Society, the ARCO Chemical Co., and a grant from the National Science Foundation (CHE-8814638). We acknowledge Lisa F. Szczepura for her assistance with the infrared isotope labeling studies and James Muller for his assistance with the collection of the NMR data.

Supplementary Material Available: Table VIII (anisotropic thermal parameters), Table IX (H atom coordinates), Figure 4 (stereoscopic view of *trans*-$[Ru(NO_2)(PMe_3)_2(trpy)](ClO_4)$ with hydrogen atoms omitted), Figure 5 ((a) proton NMR spectrum of *trans*-$[Ru(NO_2)(PMe_3)_2(trpy)](ClO_4)$ and (b) expanded region of the spectrum showing the splitting patterns for the terpyridine resonances, in $CDCl_3$, with Me_4Si as the internal reference), Figure 6 (proton-decoupled ^{13}C NMR spectrum of *trans*-$[Ru(NO_2)(PMe_3)_2(trpy)](ClO_4)$), Figure 7 (cyclic voltammograms of *trans*-$[Ru(NO_2)(PMe_3)_2(trpy)](ClO_4)$ (8 pages); a table of observed and calculated structure factor amplitudes (12 pages). Ordering information is given on any current masthead page.

(59) Simonsen, S. H.; Mueller, M. H. *J. Inorg. Nucl. Chem.* **1965**, *27*, 309.
(60) Finney, A. J.; Hitchman, M. A.; Kepert, D. L.; Raston, C. L.; Rowbottom, G. L.; White, A. H. *Aust. J. Chem.* **1981**, *34*, 2177-2187 and references therein.
(61) Seddon, E. A.; Seddon, K. R. *The Chemistry of Ruthenium*; Elsevier, New York, 1984.
(62) Clark, G. R.; Waters, J. M.; Whittle, K. R. *J. Chem. Soc., Dalton Trans.* **1975**, 2556-2560.
(63) McGuiggan, M. F.; Pignolet, L. H. *Cryst. Struct. Comm.* **1978**, *7*, 583-588.
(64) Allcock, N. W.; Raspin, K. A. *J. Chem. Soc. A* **1968**, 2108-2123.
(65) Sanchez-Delgado, R. A.; Thewalt, U.; Valencia, N.; Andriollo, A.; Marquez-Silva, R.-L.; Puga, J.; Schollhorn, H.; Klein, H.-P.; Fontal, B. *Inorg. Chem.* **1986**, *25*, 1097-1106.
(66) Robinson, S. D.; Uttley, M. F. *J. Chem. Soc., Dalton Trans* **1973**, 1912-1920.
(67) Skapski, A. C.; Stephens, F. A. *J. Chem. Soc., Dalton Trans.* **1974**, 390-395.
(68) Mason, R.; Thomas, K. M.; Gill, D. F.; Shaw, B. L. *J. Organomet. Chem.* **1972**, *40*, C67-C69.
(69) LaPlaca, S. J.; Ibers, J. A. *Inorg. Chem.* **1965**, *4*, 778-783.
(70) Leising, R. A.; Kubow, S. A.; Takeuchi, K. J. Unpublished results.